Ultrasonics - Sonochemistry 70 (2021) 105295

Contents lists available at ScienceDirect

Ultrasonics - Sonochemistry

journal homepage: www.elsevier.com/locate/ultson

Scale-up of vortex based hydrodynamic cavitation devices: A case of degradation of di-chloro aniline in water

Vivek V. Ranade[a,c,*], Varaha Prasad Sarvothaman[a], Alister Simpson[b], Sanjay Nagarajan[a], Multiphase Reactors, Intensification Group (mRING)

[a] School of Chemistry and Chemical Engineering, Queen's University Belfast, Belfast BT9 5AG, Northern Ireland, UK
[b] School of Aerospace and Mechanical Engineering, Queen's University Belfast, Belfast BT9 5AG, Northern Ireland, UK
[c] Bernal Institute, University of Limerick, Limerick, Ireland

ARTICLE INFO

Keywords:
Hydrodynamic cavitation
Vortex-based devices
Per-pass degradation
Scale-up

ABSTRACT

Hydrodynamic cavitation (HC) is being increasingly used in a wide range of applications. Unlike ultrasonic cavitation, HC is scalable and has been used at large scale industrial applications. However, no information about influence of scale on performance of HC is available in the open literature. In this work, we present for the first time, experimental data on use of HC for degradation of complex organic pollutants in water on four different scales (~200 times scale-up in terms of capacity). Vortex based HC devices offer various advantages like early inception, high cavitational yield and significantly lower propensity to clogging and erosion. We have used vortex based HC devices in this work. 2,4 dichloroaniline (DCA) – an aromatic compound with multiple functional groups was considered as a model pollutant. Degradation of DCA in water was performed using vortex-based HC devices with characteristic throat dimension, d_t as 3, 6, 12 and 38 mm with scale-up of almost 200 time based on the flow rates (1.3 to 247 LPM). Considering the experimental constraints on operating the largest scale HC device, the experimental data is presented here at only one value of pressure drop across HC device (280 kPa). A previously used per-pass degradation model was extended to describe the experimental data for the pollutant used in this study and a generalised form is presented. The degradation performance was found to decrease with increase in the scale and then plateaus. Appropriate correlation was developed based on the experimental data. The developed approach and presented results provide a sound basis and a data set for further development of comprehensive multi-scale modelling of HC devices.

1. Introduction

Hydrodynamic cavitation (HC) is a process of generation, growth and subsequent collapse of gas/vapour filled cavities leading to intense shear and hydroxyl radicals, which can be harnessed to intensify chemical and physical transformations. Several applications of HC have been reported such as: i) treatment of wastewater containing: solvent [34,30], dyes [16,21], pharmaceuticals [35] and microbes [6,18], ii) intensifying liquid–liquid reactions [14,39] and iii) pre-treatment of biomass [22,23]. Several companies are attempting to commercialise the applications of HC (for example: Biobang [4], Cavimax [10]; Cavitation Technologies [11], Dynaflow [13], Vivira Process Technologies [37]). Most of the reviews on HC primarily focus on applications [17,38,12,24]. Some of the reviews imply that the scale-up of hydrodynamic cavitation is ''relatively easy'' (for example: [17,9]) without discussing any specific evidence. There are almost no reports presenting data and performance of geometrically similar HC devices on different scales in open literature. Industrial applications on larger scales have indicated different performance on different scales [36]. We present here for the first time, experimental data of degradation of complex organic pollutants in water with geometrically similar HC devices on four different scales (up to 200 times scale-up in capacity).

HC devices are designed to realise low pressure regions in a flowing liquid where the local pressure may decrease to the vapour pressure of the liquid to generate cavitation. This can be achieved either using devices with or without moving parts. Hydrodynamic cavitation devices with moving parts, such as the rotor-stators incur higher operating and maintenance costs [15]. This work is focussed therefore on HC devices without any moving parts. Such HC devices without moving parts can be divided into subgroups based on underlying flow features used for realising cavitation: i) linear flow ii) rotational flow and (iii) their combination. Conventional HC devices are mainly based on linear

* Corresponding author at: School of Chemistry and Chemical Engineering, Queen's University Belfast, Belfast BT9 5AG, Northern Ireland, UK.
E-mail addresses: V.Ranade@qub.ac.uk, Vivek.Ranade@ul.ie (V.V. Ranade).

https://doi.org/10.1016/j.ultsonch.2020.105295
Received 4 April 2020; Received in revised form 3 June 2020; Accepted 26 July 2020
Available online 06 August 2020
1350-4177/

Nomenclature

C	Concentration of pollutants in experiments (ppm)
C_0	Starting concentration of pollutants in experiments (ppm)
C_s	Concentration of scavengers (kmol/m^3)
D1	Vortex-based cavitation device, with d_t = 3-mm
D2	Vortex-based cavitation device, with d_t = 6-mm
D3	Vortex-based cavitation device, with d_t = 12-mm
D4	Vortex-based cavitation device, with d_t = 38-mm
d_t	Throat diameter for vortex-based cavitation device (mm)
Eu	Euler number (–)
$f(n_p)$	Correction factor for changing per-pass constant (–)
G	Generation rate of hydroxyl radicals (kmol/s)
k	Turbulence kinetic energy (m^2/s^2)
k_2	Second order rate constant (M^{-1} s^{-1})
k_{app}	Pseudo first order rate constant (min^{-1})
k_s	Rate constant for scavengers (M^{-1} s^{-1})
n_p	Number of passes through cavitation device (–)
Q	Recirculating flow through cavitation device (m^3/s)
u_ω	Tangential velocity for vortex-based cavitation device (m/s)
u_t	Throat velocity for vortex-based cavitation device (m/s)
v_t	Throat velocity for vortex-based cavitation device (m/s)
V	Volume of holding tank (L)
y	Parameter indicating extent of deviation upon intermediate formation (–)
ΔP	Pressure drop across cavitation device (kPa)

Greek Symbols

β	Parameter of Equation (6)
ϒ	Parameter indicating positive or negative deviation for changing per-pass constant (–)
∅	Per-pass factor (–)
$∅_0$	Initial per-pass coefficient (–)
$∅_\infty$	Initial per-pass coefficient for infinite scale-up (–)
ρ	Liquid density (kg/m^3)
ω	Turbulence frequency (kHz)

flow in which a liquid is passed through a constriction like an orifice or venturi. The venturi and orifice based HC devices have been widely used for different applications [21,3,35,16,5]. However, venturi or orifice based devices are prone to significant erosion and clogging issues [1,31]. Devices based on rotational flows are relatively recent and do not use constrictions to realise cavitation (see for example, a vortex based cavitation device disclosed by [27]). This device differs from conventional linear flow based designs by setting up a vortex to generate cavitation so that the collapsing cavities are shielded from the reactor walls inherently by device design [31]. As demonstrated by them, it is possible to combine rotational and linear flows to generate cavitation. Though these hybrid devices show promise, these still use small constrictions and therefore are susceptible to clogging. In this work, we focus on investigating performance of vortex based cavitation devices without using small constrictions namely vortex diodes [27]. It will be useful to briefly review key aspects of realising cavitation in vortex diodes here.

The vortex diode consists of a tangential and an axial port. The fluid enters through the tangential port and exits from the axial port. The flow in a vortex diode is characterized by the conservation of angular momentum, which causes tangential acceleration of the fluid as it approaches the centre line. This sets-up a free-vortex flow in the diode chamber. This flow establishes relatively high tangential velocities, u_ω, which typically attain values of the order of 6 times that of the velocity in the throat of the tangential inlet pipe, u_t (see Fig. 1). Below a critical radius (typically about 0.12 times chamber radius), the tangential velocity is converted to the axial velocity (so that it can exit the diode) and free-vortex undergoes a transition to a "forced-vortex". This transition zone exhibits large velocity and pressure gradients near the centre. When the fluid near the axis of the device rotates with sufficiently high velocities, the corresponding local static pressure approaches vapour pressure of the fluid, causing cavitation to occur. These generated cavities are transported to the axial port where they experience a higher pressure and collapse. The collapse of cavities generates intense shear, localised high pressures and temperatures as well as hydroxyl radicals which are responsible for pollutant degradation. The flow in vortex diodes is turbulent and comprises many interacting complex flow features such as precessing vortex core (due to the asymmetric tangential port), toroidal recirculation zone, axial velocity deficit and axial port recirculating zone. Key features of vortex and turbulent flow in vortex diodes used in this work are discussed by Pandare and Ranade [25] and Simpson and Ranade [31,32] which may

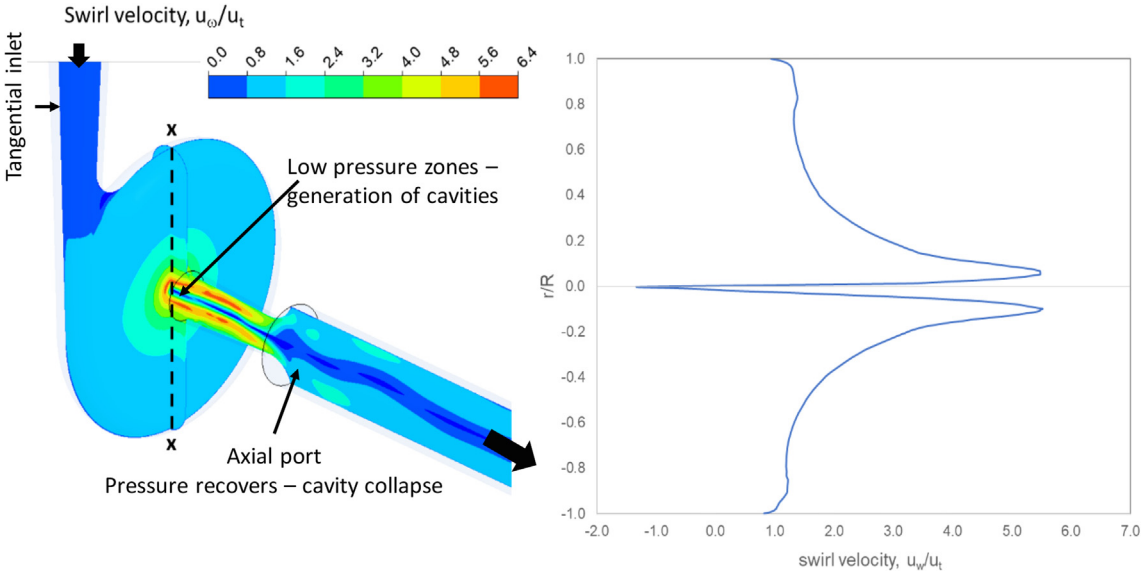

Fig. 1. Key flow characteristics of a vortex diode.

be referred for more details of these flow features. These unique flow features offer excellent opportunities for optimising hydrodynamic cavitation.

Several studies have been reported on applications of these vortex devices for variety of applications [22,30,34,33]. The device has shown significantly better cavitation performance compared to the conventional devices such as orifice [34]. In this work we present application of geometrically similar vortex based HC devices – vortex diodes for degradation of complex organic pollutant on four different scales.

Unlike previous applications of vortex based devices for degradation of pollutants in water (where simple aliphatic pollutants like acetone, ethyl acetate and isopropyl alcohol were considered – *e.g.* [29]), in this work 2,4 dichloroaniline (DCA) was used as a model pollutant. DCA has two functional groups (chlorine and amine) and an aromatic ring. Chloro-organic compounds are a class of compounds which pose environmental concern. Many industrial effluent streams contain phenol/aniline, as these two serve as a precursor to many pharmaceutical/chemical manufacturing processes. The derivative compounds of dichloroaniline find its use in the production of dyes and herbicides [19]. The DCA belong to a class of persistent environmental pollutants [2]. Application of HC using vortex based device was investigated for degrading DCA in water.

Similar to most of the studies in literature, batch experiments were carried out to study degradation of DCA in water by circulating the water through HC devices. Conventionally, such batch experimental data is interpreted using pseudo first order kinetics [26,7,28]. This is rather misleading since the degradation is not a function of time but is a function of number of passes through HC device. Sarvothaman et al. [29] have used per-pass degradation model to describe the batch experimental data of pollutant degradation. In this work, we have demonstrated that number of passes through HC device should be considered while describing degradation kinetics rather than time. The per-pass degradation model of Sarvothaman et al. [29] is extended to account for complex pollutants like DCA and a generalised formulation is presented. The model was used to interpret the performance of HC devices on four scales and a suitable correlation was established to represent observed influence of scale. The presented results will be useful for design and scale up of vortex based HC devices.

2. Experimental

The experimental setups designed for this work were similar to the hydrodynamic cavitation device based setups used in the literature [8,26,29]. Two experimental setups were designed for this work (shown schematically in Fig. 2). These were to facilitate the use of vortex-based devices on four different scales. The details of HC devices used in this work are included in the Supplementary information (Fig. S1). The characteristic dimensions of the considered four HC devices are listed in Table 1. The first experimental setup (Set-up A) was used to operate HC devices – D1, D2 and D3. A centrifugal pump with VFD (variable frequency drive) was used with this set-up (Pedrollo 4CR 80-n). The second experimental setup (Set-up B) was designed to operate the device D4. For this larger scale set-up, a centrifugal pump without VFD was used (Lowara – SHOE 32 – 200/30/D). None of these experimental setups contained a bypass line. There is always some possibility that cavitation may occur in the by-pass line (across the valves used in that line). In this work, by-pass line was eliminated to ensure that the observed pollutant degradation is because of the HC device alone. However, lack of by-pass line and lack of VFD pump for the large scale set-up (Set-up B) imposed a constraint of operation only at the pump discharge pressure, which was 280 kPa (gauge). For a systematic comparison of degradation performance on four different scales, degradation experiments on smaller scales (with Set-up A) were also carried out at HC device inlet pressure as 280 kPa (gauge). The flow rates at 280 kPa (gauge) through four HC devices are listed in Table 1. It can be seen that the flow rate of the largest device is almost 200 times larger than that for the smallest device. The liquid volume used in the holding tank for these four HC devices is also listed in Table 1 so that number of passes and elapsed time can be related to each other. Photographs of the experimental set-ups are shown in Figure S2a and S2b.

Pre-calibrated analogue pressure gauges procured from Thermosense Direct (P1, downstream of the pump; P2, upstream of the cavitation device and P3, downstream of the cavitation device) in the ranges of 0–700; 0–400 kPa and 0–100 kPa respectively were used to monitor the pressure. The vortex-based cavitation devices were manufactured in stainless steel were procured from Vivira Process Technologies (www.vivira.in). In typical experiments, tap water with a calculated quantity of DCA was recirculated through the cavitation setup shown in Fig. 2 to ensure that the initial concentration was nearly 0.035 g/L (35 ppm). Cooling water was circulated with the help of a stainless steel cooling coil to ensure that the temperature was maintained at room temperature, all the experiments reported were all performed at room temperature, unless specified. The degradation experiments were performed in triplicates. The experiments were performed at room temperature (18 °C) and the variation in temperature for these experiments was within ± 2 °C.

The stock solution of DCA was prepared by dissolving nearly 25 g of the pure compound (procured from TCI UK Ltd.) was powdered using a clean mortar-pestle and the powdered DCA was then dissolved in a 20-L of bucket of water (more than the solubility limit). Overhead stirring was provided to the solution and this assembly was left overnight. After the overnight dissolution and stirring, the nearly saturated solution of DCA with undissolved solids was vacuum filtered to remove the undissolved solids. The nearly saturated solution (~1 g/L) was collected and stored for cavitation experiments. The initial concentration of DCA for cavitation experiments was chosen to ensure that the intensity of the peak at the wavelength on UV–Vis spectroscopy of 241 nm peak was 1.0 (UV–Vis spectrophotometer from Shimadzu - UV 1280) and to ensure that no dilution of samples was required during analysis. A standard curve was plotted as absorbance at 241 nm against DCA concentration. The equation obtained from the standard curve was used to determine the concentration of the unknown sample obtained from subsequent cavitation experiments. A sample of UV spectrum and calibration curve are included as Fig. S3 in the Supplementary Information. Control experiments were carried out to ensure that no degradation of DCA occurs in absence of cavitation (see Fig. S4).

3. Results and discussion

3.1. Preliminary investigations

Before proceeding to the pollutant degradation experiments using the vortex based HC devices, it was decided to carry out preliminary studies primarily on pressure drop characteristics of the considered devices, influence of initial concentration of pollutant and influence of

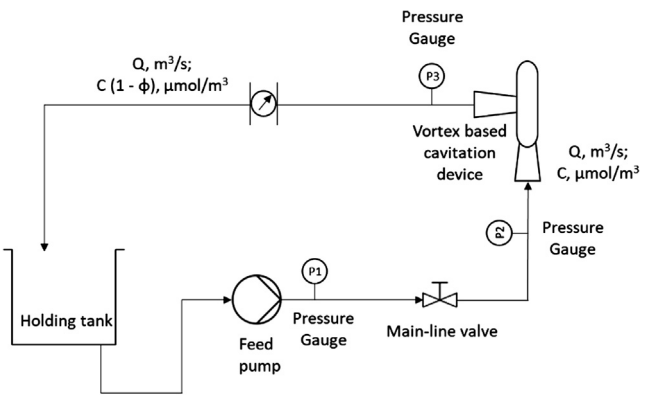

Fig. 2. Schematic of experimental setup used in this study.

Table 1
Flow rate and dimensions of cavitation devices used in this study.

Diode name	Characteristic dimension of vortex based cavitation device – d_t (mm)	Flow at ΔP = 280 kPa, LPM	Liquid volume, L
D1	3	1.3	3
D2	6	5.0	3
D3	12	19.5	5
D4	38	247.6	80

liquid volume in the holding tank. The data on pressure drop across HC devices for a range of flow rates was obtained for devices D1, D2 and D3 using the experimental Set-up A. The throat diameter, d_t (see Fig. S1 and Table 1) of vortex-based devices was used as a characteristic dimension. Flow rates through cavitation devices were measured across the pressure drop range of 50 to 350 kPa across the three scales (in triplicate). The experimental data is shown in Fig. 3. The data can be represented adequately using the following equation:

$$\Delta P = Eu\frac{1}{2}\rho v_t^2 \tag{1}$$

The value of Euler number was found to be 60, for the three devices used in the present study (see Fig. 3). The same value was found to describe data from an earlier study with vortex based devices [20]. The pressure drop data reported by Kulkarni et al. [20] for three different devices (d_t = 6/9 and 25-mm) was also shown in Fig. 3. The present data as well as published data may indicate a slight increase in the value of Eu as the size of the device is increases. The available data however is not adequate to propose a definitive relationship. At the moment, therefore, it may be said that the pressure drop for these devices used in the current study and published literature [20] can be represented by Eu = 60. There is a possibility that the value may increase to some extent as the size of the HC device increases.

The next parameter studied was the initial concentration. These experiments were carried out with the device D2. In the experimental section, the initial concentration (C_0) was mentioned as 35 ppm. Three different concentrations were used in these experiments: 0.5 C_0, C_0 and 2 C_0. The observed degradation profiles are shown in Fig. 4. It can be seen that in the tested range of initial concentration, the degradation profiles did not show any influence on degradation performance. For clearly understanding the role of number of passes through HC device on pollutant degradation, volume of liquid in the holding tank was varied. These experiments were carried out with device, D3. Degradation of DCA was quantified for holding tank containing two different liquid volumes: 0.005 and 0.024 m^3. Three experiments were performed with the 0.005 m^3 (5 L) liquid volume and an experiment was performed with 0.024 m^3 (24 L) liquid volume. The observed DCA concentration profiles (dimensionless) are shown as a function of time (in Fig. 5a) and of number of passes through HC device (in Fig. 5b). It can be seen that concentration profiles with respect to time for two different liquid volumes in the holding tank differ from each other – leading to two different values of effective degradation rate constant (k_{app} = 1.06 × 10^{-3} min^{-1} for 0.005 m^3 and k_{app} = 2.41 × 10^{-4} min^{-1} for 0.024 m^3). It should be noted that the performance of HC device operated at same flow rate is not expected to be a function of liquid volume in the holding tank! Unlike this, the observed degradation profile with respect to number of passes for the experiment with higher liquid volume lies within the replicates of the lower liquid volume – indicating similar performance of HC device in both the cases. This indicates that it is more appropriate to interpret the observed concentration degradation profiles using the per-pass degradation factor rather than using pseudo first order rate constant.

3.2. Extended per-pass degradation model to interpret DCA data

As discussed in previous section, it is more appropriate to interpret the observed pollutant degradation data using the per-pass degradation model. Recently, Sarvothaman et al. [29] have simplified the pollutant degradation reactions as:

Cavity collapse → $OH^{\cdot}$ *and other radicals* ($R^{\cdot}$) (R 1)

$R^{\cdot}$ + *pollutant* → $CO_2 + H_2O$ (R 2)

An attempt was therefore made to use the constant per-pass model to describe the degradation of DCA in water. The data collected with a smallest device (D1) was used for this purpose. The comparison of the best fit with respect to experimental data is shown in Fig. 6 (solid curve marked with y = 0). It can be seen that the fit is not good. The observed disagreement between constant per-pass degradation factor and experimental data indicates the possibility of non-constant per-pass degradation factor. It should be noted that DCA is a complex molecule compared to simple model pollutants considered by Sarvothaman et al. [29]. Complete mineralisation of pollutants like DCA proceeds via a multi-step unstable organic radical reactions. There are several attempts to understand radical formation and their subsequent reactions with pollutants (see for example reaction schemes proposed by [28]). Detailed accounting of underlying radical reactions is not possible and may not be necessary. Instead, in this work, the reaction R2 is broken into two parts:

$R^{\cdot}$ + *pollutant* → *Intermediates* (R 3)

$R^{\cdot}$ + *Intermediates* → $CO_2 + H_2O$ (R 4)

The reactivity of intermediate products may be different from the original pollutant and may change effective per pass degradation factor. This will be especially relevant when radical production rate is relatively low and observed change in the pollutant concentration is significant. To account for such variation in per-pass degradation factor, Eq. (1) may be rewritten as:

$$\frac{dC}{dn_p} = -\emptyset_0 f(n_p)C \tag{2}$$

where ϕ_0 is initial per-pass degradation factor and $f(n_p)$ is a correction factor to account for varying ϕ over number of passes (as the pollutant degrades to mineralisation via multiple steps). Various possible functions for correction factor were considered. For maintaining the consistent formulation from n_p = 0, the following equation was finalised for the correction factor:

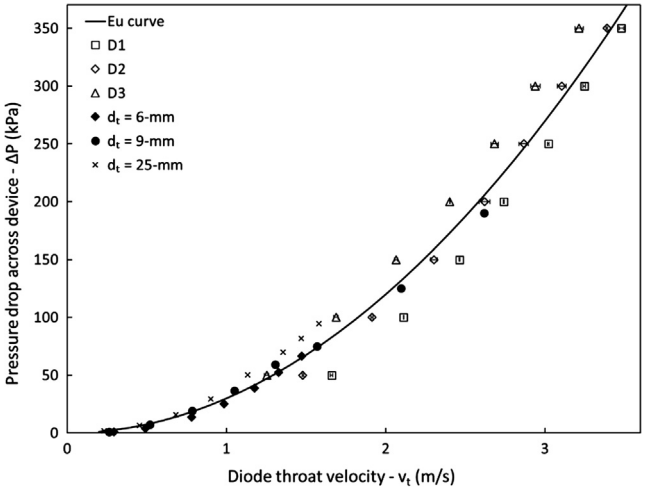

Fig. 3. Pressure drop and flow relationships for vortex based cavitation devices. Symbols: experimental data, Lines: Euler number = 60. HC devices from the current study: D1, D2 and D3; Devices from [20]: d_t = 6-mm, d_t = 9-mm and d_t = 25-mm.

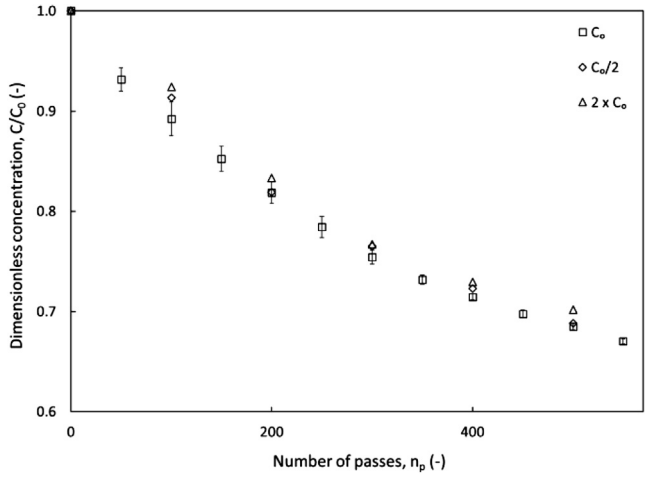

Fig. 4. Influence of initial concentration on degradation performance, HC device – D2, (V) = 3 L.

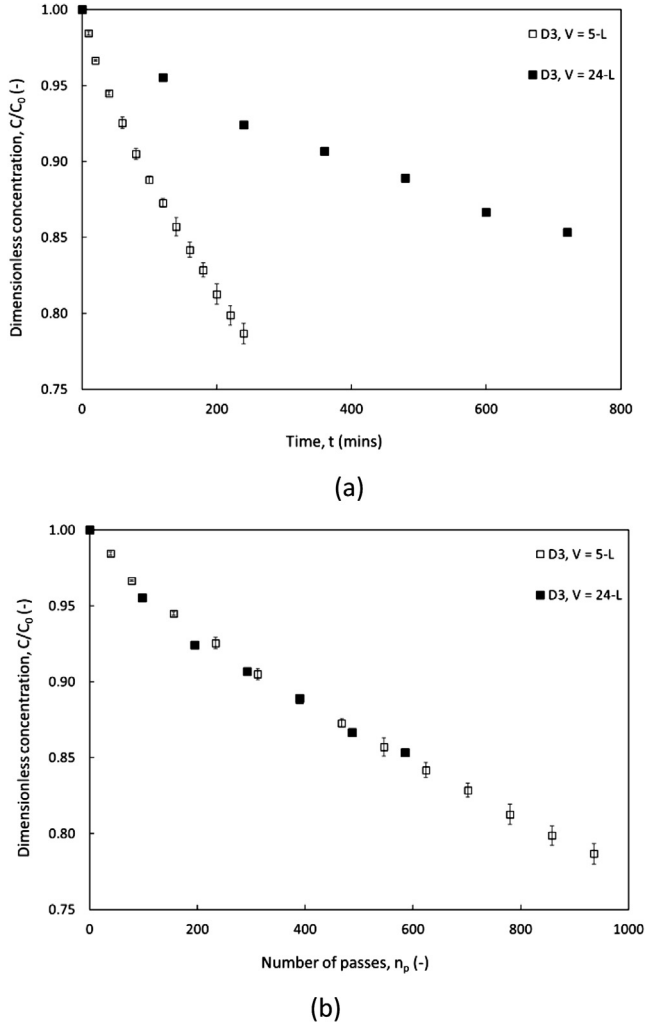

Fig. 5. Influence of liquid volume on degradation performance, HC device – D3, ΔP: 280 kPa Liquid volume in the holding tank, V: open square – 0.005 m^3, filled square – 0.024 m^3 (a) Profile with respect to time and (b) Profile with respect to number of passes.

$$f(n_p) = \frac{1}{(1 + \gamma \varnothing_0 n_p)^y} \tag{3}$$

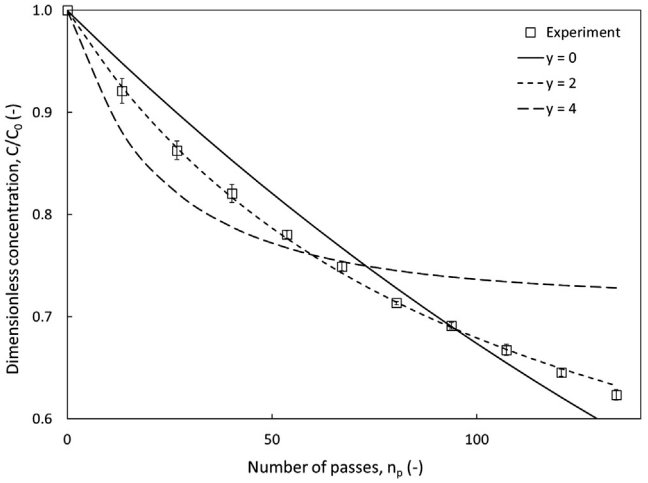

Fig. 6. Application of per-pass degradation model to the degradation of DCA data [HC device D1, ΔP = 280 kPa].

The value of parameter, y as zero will reduce this function to unity and the model will reduce to the simple, constant per-pass degradation factor identical to the one proposed in our earlier study [29]. If the intermediates formed are more reactive than the original pollutant, the ϒ in Eq. (3) will have positive sign leading to reduction in per-pass degradation factor with subsequent number of passes. If the intermediates formed are less reactive than the original pollutant, the ϒ in Eq. (3) may have negative sign leading to increase per-pass degradation factor with subsequent number of passes. The presence of ϕ_0 in the denominator indicates that larger the value of per-pass degradation factor, higher is the impact of different reactivity of intermediates. The empirical parameter 'y' controls the extent of influence of different reactivity of intermediates.

Substituting Eq. (3) in Eq. (2) and integrating we get (for y ≠ 1),

$$ln\left(\frac{C}{C_0}\right) = -\varnothing_0\left[\frac{(1 + \gamma \varnothing_0 n_p)^{y-1} - 1}{\varnothing_0 (y-1)(1 + \gamma \varnothing_0 n_p)^{y-1}}\right] \tag{4}$$

The equation thus contains three parameters, per-pass degradation factor, ϕ_0; ϒ which indicates the sign of change of per pass degradation factor with number of passes and parameter y which indicates the severity of the change. For the case of degradation of DCA (see data shown in Fig. 6), it was observed that intermediates produced are more reactive and thus the sign in the denominator was taken as positive (ϒ = +1). Different values of 'y' were evaluated. It can be seen from Fig. 6 that y = 2 was able to describe the degradation data adequately. For all subsequent data processing, the following equation was used to fit the observed DCA concentration profile:

$$\left(\frac{C}{C_0}\right) = e^{-\varnothing_0 n_p/(1+\varnothing_0 n_p)} \tag{5}$$

This Eq. (5) was found to describe the experimental degradation data quite well and therefore was used for investigating influence of device scale on degradation performance.

3.3. Influence of device scale on degradation performance

The observed DCA degradation data for larger HC devices (D2, D3 and D4) were fitted using Eq. (5) as shown in Fig. 7. It can be seen that Eq. (5) was able to describe the DCA degradation data for all the four HC devices. The values of $ø_0$ obtained through these fitting are listed in Table 2. It can be seen that the values of initial per-pass degradation factor decreases with increase in device scale. It will be instructive to look at the overall cavitation performance on different scales.

It can be seen that initial degradation rate is highest for the largest

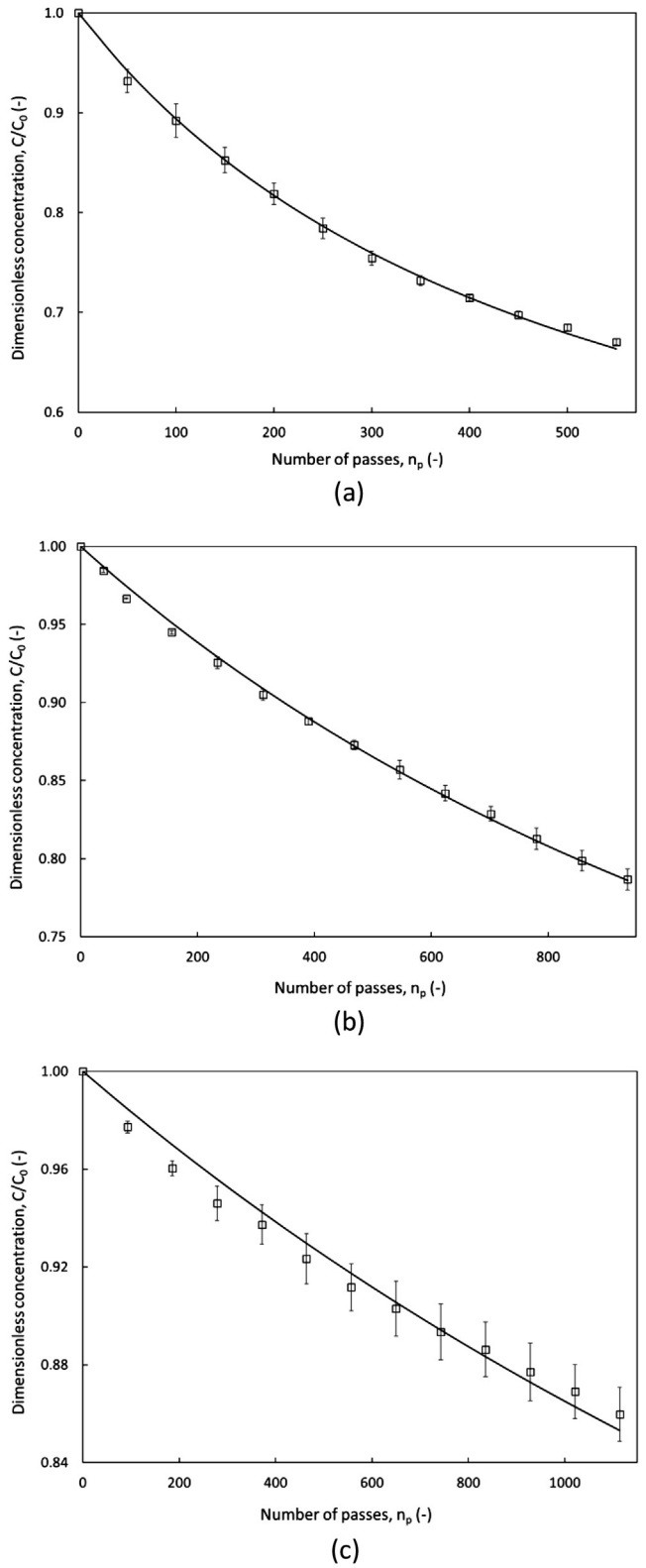

Fig. 7. Degradation profile at 280-kPa for devices (a) D2, (b) D3 and (c) D4. Symbols: experimental data, and Lines: predictions using Eq. (5), values of $ø_0$ used are listed in Table 2. Details of devices mentioned in Table 1.

HC device, D4 (more than 700 μg/hr). The initial degradation rates for the three smaller HC devices (D1, D2 and D3) are more or less same and less than 140 μg/hr (see Fig. 8). The initial degradation rate per unit energy consumption however shows a different picture. The smallest HC device shows the best performance in terms of degradation per unit energy consumption which continuously decreases with increase in the scale of HC device. The average degradation rates over 100 passes also show similar trend.

Based on these experimental results, an attempt is made to develop a correlation for $ø_0$ as a function of device scale. The observed initial per-pass degradation factor, $ø_0$, for DCA in water (see Fig. 9) may be represented by Eq. (6):

$$\varnothing_0 = \varnothing_\infty \exp\left(\frac{\beta}{d_t}\right) \tag{6}$$

The values of estimated $ø_0$ using the data from three replicated experiments obtained on four HC device scales at pressure drop across device as 280 kPa was used to calculate values of two parameters appearing in Eq. (6): $ø_\infty$ and β. As mentioned earlier, the degradation performance was found to decrease with the HC device scale. The observed data however indicates that it plateaus and exhibits a finite initial per-pass degradation factor for the infinitely large HC device, $ø_\infty$. The value of $ø_\infty$ found to be 1.5×10^{-4} while the value of β was found to be 10.85. The comparison of observed DCA degradation profiles with those estimated based on Eqs. (5) and (6) is shown in Fig. 10. The observed agreement between the experimental data and predicted results over four scales was found to be inferior to those obtained for individual device scale (Figs. 6 and 7). Use of two parameter equation (Eq. (6)) for describing data of four scales of devices inevitably introduced some errors. These errors were found to be larger for device D2 compared to the other devices (D1, D3 and D4). It is possible to improve the fit by introducing additional parameter in the correlation. However, considering that the experimental data was available only at four scales, it was prudent to not increase number of parameters to more than two. It is possible to force better fit to device D2. However, this will lead to inferior fit to other devices. The parameter values of $ø_\infty = 1.5 \times 10^{-4}$ and $\beta = 10.85$ were found to be best choice. Considering the 200-fold variation in the flow rates, the overall agreement between the experimental data of DCA degradation and predictions using Eqs. (5) and (6) is found to be reasonable and adequate.

Considering that characteristic life time of generated hydroxyl radicals will not change with change in HC device scale, some impact of HC device scale on degradation performance of geometrically similar HC devices is expected. The overall performance of a HC device is dictated by different phenomena such as cavity generation rate, size distributions, the interaction of cavities with the flow and neighbouring cavities [32]. A simple dimensional analysis indicates the following trends of volume averaged turbulent quantities in HC devices:

$$k \propto v_t^2 \tag{7}$$

$$\omega \propto \frac{v_t}{d_t} \tag{8}$$

Turbulent kinetic energy, k and specific turbulent dissipation rate, ω determine the amplitude and frequency of pressure fluctuations experienced by cavities which will ultimately influence collapse intensity. In principle it is possible to use a multi-scale approach presented by Sarvothaman et al. [30] which combine cavity dynamics models and detailed computational fluid dynamic models of HC devices to interpret the influence of scale. The application of such an approach to simulate the results presented here is in progress and will be presented separately. The results presented here at a fixed pressure drop across HC device at four different scales will provide crucial basis for validation of multi-scale models and for providing scale-up guidelines.

4. Summary and conclusions

In this work we have investigated performance of vortex based HC devices for degradation of DCA in water – a complex organic pollutant with aromatic ring with two chlorine and amine groups. For the first time, experimental results on four geometrically similar HC devices

Table 2
Influence of HC device scale on DCA degradation performance (*Calculations are based on hypothetical concentration of 1000 ppm).

Diode name	Initial per-pass degradation factor, $\phi_0 \times 10^5$	Initial degradation rate, μg/h*	Initial degradation rate, μg/hr*/W	Average degradation over 100 passes, μg/J
D1	632.4	137	81,308	4130
D2	126.4	105	16,251	1365
D3	33.9	110	4358	415
D4	17.0	701	2185	213

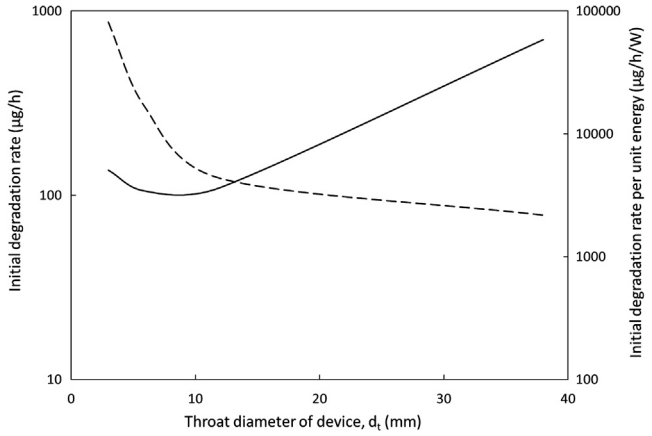

Fig. 8. Influence of HC device scale on cavitation performance.

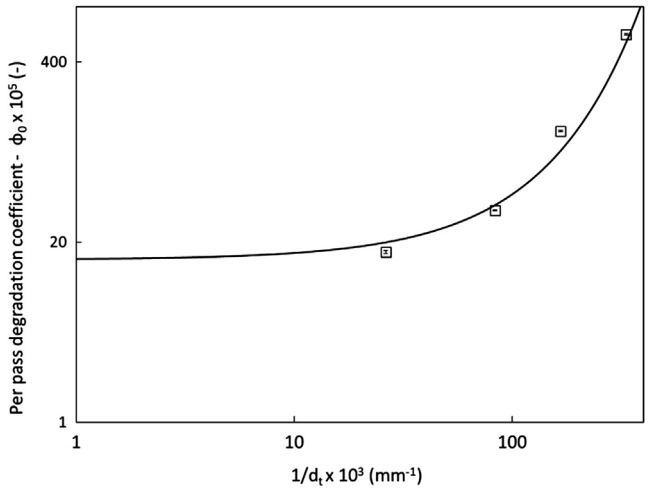

Fig. 9. Influence of HC device scale on initial per-pass degradation factor for DCA.

spanning a scale-up of nearly 200 times are presented. The degradation of DCA was interpreted by extending a previously developed per-pass modelling. The degradation experiments were performed at an identical pressure drop condition: 280 kPa for these four different scales. Preliminary experiments were performed to understand the flow characteristics of these devices and to understand the role of initial concentration on degradation. Experiments were performed to confirm the necessity of per-pass degradation by varying liquid volume. This extended per-pass degradation coefficient was used to develop a correlation for degradation performance with device scale. The key conclusions from the study are as follows:

- Pressure drop of vortex based HC devices used in this study could be represented by Eu = 60 which is consistent with the published literature.
- The degradation profile for DCA was found to be independent of initial concentration of the pollutant in the ranges of 17.5 to 70 ppm.
- The experimental result for different operating volumes at identical flow through HC device clearly bring out necessity of using per-pass models over pseudo first order kinetics approach.
- The extended per-pass degradation factor (Eq. (5)) was able to suitably describe experimental data of DCA degradation.
- Degradation performance was found to decrease with increase in device scale with a finite limiting value for infinite scale-up. A simple exponential relationship between per-pass degradation and inverse of throat diameter (Eq. (6)) was found to describe the influence of scale adequately.

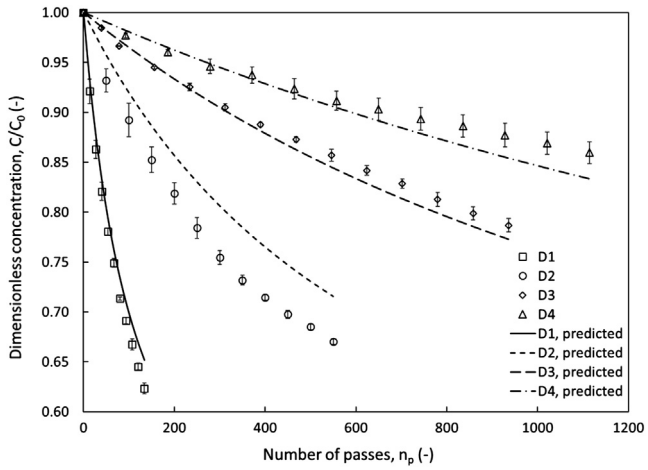

Fig. 10. Comparison of experimental data with those predicted using Eqs. (5) and (6).

The generalised per-pass degradation model presented here (Eq. (4)) will be useful to describe degradation of complex organic pollutants using hydrodynamic cavitation. The presented experimental data provides a sound basis for development and validation of multi-layer models for scale-up of vortex based HC devices. The results will be useful to researchers as well as practicing engineers in expanding application of hydrodynamic cavitation for effluent treatment.

CRediT authorship contribution statement

Vivek V. Ranade: Conceptualization, Funding acquisition, Supervision. **Varaha Prasad Sarvothaman:** Investigation, Data curation, Validation. **Alister Simpson:** Investigation, Validation. **Sanjay Nagarajan:** Investigation, Validation. **:** .

Declaration of Competing Interest

The authors declare the following financial interests/personal relationships which may be considered as potential competing interests: One of the authors (VVR) is a Director of Vivira Process Technologies Pvt., Ltd., which commercially offers the vortex-based cavitation devices used in this study.

Acknowledgement

The authors gratefully acknowledge funding support from the start-up Grant G1013CHM from Queen's University Belfast, United Kingdom; and Innovate UK, BBSRC UK and Department of Biotechnology, Government of India for funding the vWa Project (BBSRC Grant Ref: BB/S011951/1). The authors gratefully acknowledge the useful contribution (wiring of three phase pumps used in the study) of Kirin Hill toward this work.

Declaration of interests

One of the authors (VVR) is a Director of Vivira Process Technologies Pvt., Ltd., which commercially offers the vortex-based cavitation devices used in this study.

Appendix A. Supplementary data

Supplementary data to this article can be found online at https://doi.org/10.1016/j.ultsonch.2020.105295.

References

[1] L. Albanese, R. Ciriminna, F. Meneguzzo, M. Pagliaro, Gluten reduction in beer by hydrodynamic cavitation assisted brewing of barley malts, LWT-Food Sci. Technol. 82 (2017) 342–353.
[2] T.S. Alkhuraiji, W.S. Alkhuraiji, Detailed study of water radiolysis-based degradation of chloroorganic pollutants in aqueous solutions, J. Hazard. Mater. 368 (2019) 569–577.
[3] K.O. Badmus, J.O. Tijani, E. Massima, L. Petrik, Treatment of persistent organic pollutants in wastewater using hydrodynamic cavitation in synergy with advanced oxidation process, Environ. Sci. Pollut. Res. 25 (8) (2018) 7299–7314.
[4] Biobang, 2019, https://www.biobang.com, last accessed: 9th January 2020.
[5] P. Braeutigam, M. Franke, R.J. Schneider, A. Lehmann, A. Stolle, B. Ondruschka, Degradation of carbamazepine in environmentally relevant concentrations in water by Hydrodynamic-Acoustic-Cavitation (HAC), Water Res. 46 (7) (2012) 2469–2477.
[6] E. Burzio, F. Bersani, G.C.A. Caridi, R. Vesipa, L. Ridolfi, C. Manes, Water disinfection by orifice-induced hydrodynamic cavitation, Ultrason. Sonochem. 104740 (2019).
[7] M. Capocelli, D. Musmarra, M. Prisciandaro, A. Lancia, Chemical effect of hydrodynamic cavitation: simulation and experimental comparison, AIChE J. 60 (7) (2014) 2566–2572.
[8] M. Capocelli, M. Prisciandaro, A. Lancia, D. Musmarra, Hydrodynamic cavitation of p-nitrophenol: a theoretical and experimental insight, Chem. Eng. J. 254 (2014) 1–8.
[9] J. Carpenter, M. Badve, S. Rajoriya, S. George, V.K. Saharan, A.B. Pandit, Hydrodynamic cavitation: an emerging technology for the intensification of various chemical and physical processes in a chemical process industry, Rev. Chem. Eng. 33 (5) (2017) 433–468.
[10] Cavimax, 2019, http://www.cavimax.co.uk, last accessed: 9th January 2020.
[11] Cavitation Technologies, 2019, http://www.ctinanotech.com, last accessed: 9th January 2020.
[12] M. Dular, T. Griessler-Bulc, I. Gutierrez-Aguirre, E. Heath, T. Kosjek, A.K. Klemenčič, M. Oder, M. Petkovšek, N. Rački, M. Ravnikar, A. Šarc, Use of hydrodynamic cavitation in (waste) water treatment, Ultrason. Sonochem. 29 (2016) 577–588.
[13] Dynaflow, 2019, http://www.dynaflow-inc.com, last accessed: 9th January 2020.
[14] M. Farvardin, B. Hosseinzadeh Samani, S. Rostami, A. Abbaszadeh-Mayvan, G. Najafi, E. Fayyazi, Enhancement of biodiesel production from waste cooking oil: ultrasonic-hydrodynamic combined cavitation system, Energy Sources, Part A: Recov. Utiliz. Environ. Effects (2019) 1–15.
[15] P.R. Gogate, A.B. Pandit, Hydrodynamic cavitation reactors: a state of the art review, Rev. Chem. Eng. 17 (1) (2001) 1–85.
[16] M.M. Gore, V.K. Saharan, D.V. Pinjari, P.V. Chavan, A.B. Pandit, Degradation of reactive orange 4 dye using hydrodynamic cavitation based hybrid techniques, Ultrason. Sonochem. 21 (3) (2014) 1075–1082.
[17] C.R. Holkar, A.J. Jadhav, D.V. Pinjari, A.B. Pandit, Cavitationally driven transformations: A technique of process intensification, Ind. Eng. Chem. Res. 58 (15) (2019) 5797–5819.
[18] P. Jain, V.M. Bhandari, K. Balapure, J. Jena, V.V. Ranade, D.J. Killedar, Hydrodynamic cavitation using vortex diode: An efficient approach for elimination of pathogenic bacteria from water, J. Environ. Manage. 242 (2019) 210–219.
[19] Kahl, T., Schröder, K.W., Lawrence, F.R., Marshall, W.J., Höke, H. and Jäckh, R., 2000. Aniline. Ullmann's Encyclopedia of Industrial Chemistry.
[20] A.A. Kulkarni, V.V. Ranade, R. Rajeev, S.B. Koganti, CFD simulation of flow in vortex diodes, AIChE J. 54 (5) (2008) 1139–1152.
[21] M.S. Kumar, S.H. Sonawane, B.A. Bhanvase, B. Bethi, Treatment of ternary dye wastewater by hydrodynamic cavitation combined with other advanced oxidation processes (AOP's), J. Water Process Eng. 23 (2018) 250–256.
[22] S. Nagarajan, V.V. Ranade, Pretreatment of Lignocellulosic Biomass Using Vortex-Based Devices for Cavitation: Influence on Biomethane Potential, Ind. Eng. Chem. Res. 58 (35) (2019) 15975–15988.
[23] K. Nakashima, Y. Ebi, N. Shibasaki-Kitakawa, H. Soyama, T. Yonemoto, Hydrodynamic cavitation reactor for efficient pretreatment of lignocellulosic biomass, Ind. Eng. Chem. Res. 55 (7) (2016) 1866–1871.
[24] J. Ozonek, Application of Hydrodynamic Cavitation In Environmental Engineering, CRC Press, 2012.
[25] A. Pandare, V.V. Ranade, Flow in vortex diodes, Chem. Eng. Res. Des. 102 (2015) 274–285.
[26] S. Rajoriya, S. Bargole, V.K. Saharan, Degradation of a cationic dye (Rhodamine 6G) using hydrodynamic cavitation coupled with other oxidative agents: Reaction mechanism and pathway, Ultrason. Sonochem. 34 (2017) 183–194.
[27] Ranade, V.V., Kulkarni, A.A. and Bhandari, V.M., Council of Scientific and Industrial Research (CSIR), 2017. Apparatus and method for reduction in ammoniacal nitrogen from waste waters. U.S. Patent 9,725,338.
[28] V.K. Saharan, D.V. Pinjari, P.R. Gogate, A.B. Pandit, Advanced oxidation technologies for wastewater treatment: an overview, Industrial Wastewater Treatment, Recycling and Reuse, Elsevier, 2014, pp. 141–191.
[29] V.P. Sarvothaman, S. Nagarajan, V.V. Ranade, Treatment of solvent-contaminated water using vortex-based cavitation: influence of operating pressure drop, temperature, aeration, and reactor scale, Ind. Eng. Chem. Res. 57 (28) (2018) 9292–9304.
[30] V.P. Sarvothaman, A.T. Simpson, V.V. Ranade, Modelling of vortex based hydrodynamic cavitation reactors, Chem. Eng. J. 377 (2019) 119639.
[31] A. Simpson, V.V. Ranade, 110th Anniversary: comparison of cavitation devices based on linear and swirling flows: hydrodynamic characteristics, Ind. Eng. Chem. Res. 58 (31) (2019) 14488–14509.
[32] A. Simpson, V.V. Ranade, Flow characteristics of vortex based cavitation devices: Computational investigation on influence of operating parameters and scale, AIChE J. 65 (9) (2019) 16675.
[33] N.B. Suryawanshi, V.M. Bhandari, L.G. Sorokhaibam, V.V. Ranade, Developing techno-economically sustainable methodologies for deep desulfurization using hydrodynamic cavitation, Fuel 210 (2017) 482–490.
[34] P.G. Suryawanshi, V.M. Bhandari, L.G. Sorokhaibam, J.P. Ruparelia, V.V. Ranade, Solvent degradation studies using hydrodynamic cavitation, Environ. Prog. Sustainable Energy 37 (1) (2018) 295–304.
[35] P. Thanekar, M. Panda, P.R. Gogate, Degradation of carbamazepine using hydrodynamic cavitation combined with advanced oxidation processes, Ultrason. Sonochem. 40 (2018) 567–576.
[36] Utikar, R.P. (2019), Private communications.
[37] Vivira Process Technologies Ltd, 2019, http://www.vivira.in, last accessed: 9th January 2020.
[38] A. Waghmare, K. Nagula, A. Pandit, S. Arya, Hydrodynamic cavitation for energy efficient and scalable process of microalgae cell disruption, Algal Res. 40 (2019) 101496.
[39] Z. Wu, T. Zheng, L. Wu, H. Lou, Q. Xie, M. Lu, L. Zhang, Y. Nie, J. Ji, Novel reactor for exothermic heterogeneous reaction systems: Intensification of mass and heat transfer and application to vegetable oil epoxidation, Ind. Eng. Chem. Res. 56 (18) (2017) 5231–5238.